Carpenter syndrome: extended RAB23 mutation spectrum and analysis of nonsense-mediated mRNA decay

Andrew Om Wilkie, Dagan Jenkins, Gareth Baynam, Luc de Catte, Nursel Elcioglu, Michael Gabbett, Louanne Hudgins, Jane A Hurst, Fernanda Sarquis Jehee, Christine Oley

Human Mutation

Carpenter syndrome: extended RAB23 mutation spectrum and analysis of nonsense-mediated mRNA decay

Journal:	*Human Mutation*
Manuscript ID:	humu-2010-0523.R1
Wiley - Manuscript type:	Mutation in Brief
Date Submitted by the Author:	16-Dec-2010
Complete List of Authors:	Wilkie, Andrew; Weatherall Institute of Molecular Medicine Jenkins, Dagan; University of Oxford, WIMM Baynam, Gareth; University of Western Australia, Genetic Services of Western Australia De Catte, Luc; University Hospital Gasthuisberg, Obstetrics and Gynecology Elcioglu, Nursel; Marmara University Medical Faculty, Department of Pediatric Genetics Gabbett, Michael; The University of Queensland, Royal Brisbane & Women's Hospital Hudgins, Louanne; Stanford University, Division of Medical Genetics Hurst, Jane; Oxford Radcliffe Hospitals, Clinical Genetics Jehee, Fernanda; Universidade de São Paulo, Departamento de Genética e Biologia Evolutiva Oley, Christine; Birmingham women hospital
Key Words:	acrocephalopolysyndactyly, nonsense mediated mRNA decay, point mutation, switch domain, polydactyly, craniosynostosis

HUMAN MUTATION Mutation in Brief #____ (20XX) Online

MUTATION IN BRIEF

HUMAN MUTATION

Carpenter syndrome: extended *RAB23* mutation spectrum and analysis of nonsense-mediated mRNA decay

OFFICIAL JOURNAL HGVS HUMAN GENOME VARIATION SOCIETY www.hgvs.org

Dagan Jenkins [1], Gareth Baynam [2], Luc De Catte [3], Nursel Elcioglu [4], Michael T. Gabbett [5,6], Louanne Hudgins [7], Jane A. Hurst [8], Fernanda Sarquis Jehee [9], Christine Oley [10], Andrew O. M. Wilkie [1,8]

[1] Weatherall Institute of Molecular Medicine, University of Oxford, John Radcliffe Hospital, Oxford, United Kingdom; [2] Genetic Services of Western Australia, Princess Margaret Hospital for Children and King Edward Memorial Hospital for Women, School of Paediatrics and Child Health, University of Western Australia, Perth, Australia; [3] Department of Obstetrics and Gynecology, University Hospital Gasthuisberg, Leuven, Belgium; [4] Department of Pediatric Genetics, Marmara University Medical Faculty, Istanbul, Turkey; [5] Royal Brisbane & Women's Hospital and [6] The University of Queensland, Brisbane, Australia; [7] Division of Medical Genetics, Department of Pediatrics, Stanford University, Stanford CA, USA; [8] Department of Clinical Genetics, Oxford Radcliffe Hospitals NHS Trust, Oxford, United Kingdom; [9] Centro de Estudos do Genoma Humano, Departamento de Genética e Biologia Evolutiva, Universidade de São Paulo, São Paulo, Brazil; [10] West Midlands Regional Genetics Service, Birmingham Women's Healthcare NHS Trust, Birmingham, United Kingdom

*Correspondence to Andrew O. M. Wilkie, Weatherall Institute of Molecular Medicine, University of Oxford, John Radcliffe Hospital, Oxford OX3 9DS, United Kingdom. awilkie@hammer.imm.ox.ac.uk

Contract grant sponsor: Medical Research Council; Contract grant number: 80186. Wellcome Trust; Contract grant number: 078666.

Short Title: *RAB23* mutations and nonsense mediated decay.

Communicated by <Please don't enter>

ABSTRACT: Carpenter syndrome, a rare autosomal recessive disorder characterized by a combination of craniosynostosis, polysyndactyly, obesity, and other congenital malformations, is caused by mutations in *RAB23*, encoding a member of the Rab-family of small GTPases. In 15 out of 16 families previously reported, the disease was caused by homozygosity for truncating mutations, and currently only a single missense mutation has been identified in a compound heterozygote. Here, we describe a further 8 independent families comprising 10 affected individuals with Carpenter syndrome, who were positive for mutations in *RAB23*. We report the first homozygous missense mutation and in-frame deletion, highlighting key residues for RAB23 function, as well as the first splice-site mutation. Multi-suture craniosynostosis and polysyndactyly have been present in all patients described to date, and abnormal external genitalia have been universal in boys. High birth weight was not evident in the current group of patients, but further evidence for laterality defects is reported. No genotype-phenotype correlations are apparent. We provide experimental evidence that transcripts encoding truncating mutations are subject to nonsense-mediated decay, and that this plays an important role in the pathogenesis of many *RAB23*

Received <date>; accepted revised manuscript <date>.

mutations. These observations refine the phenotypic spectrum of Carpenter syndrome and offer new insights into molecular pathogenesis. ©2010 Wiley-Liss, Inc.

KEY WORDS: *RAB23*; acrocephalopolysyndactyly syndrome; nonsense mediated mRNA decay; point mutations; switch domain

INTRODUCTION

Carpenter syndrome (MIM #201000), a classical autosomal recessive multiple congenital malformation disorder first described in 1901 [Carpenter, 1901], is characterized by craniosynostosis, polysyndactyly, obesity and other malformations. We previously reported that Carpenter syndrome is caused by mutations in *RAB23* (MIM *606144), encoding a member of the Rab-family of small GTPases involved in vesicle trafficking [Jenkins et al., 2007]. Since then, there has been a single confirmatory study describing a novel homozygous frameshift mutation in one family [Alessandri et al., 2010]. Because of a significant founder effect, with affected individuals in 10 out of 16 mutation-positive families being homozygous for a single mutation (c.434T>A encoding p.L145X, present on an apparently shared haplotype), the spectrum of described mutations in *RAB23* is limited. The collated *RAB23* mutation data document homozygosity for five different truncating mutations (three associated with frameshifts and two encoding nonsense codons) in all but one of the 16 families reported to date; the final affected individual being a compound heterozygote for p.L145X and a predicted missense mutation, p.C85R [Jenkins et al., 2007; Alessandri et al., 2010]. Currently it is unclear whether the lack of homozygous missense mutations is a chance observation or possibly reflects a distinct functional effect of such mutations, leading to a different phenotype.

All Rab proteins have the same arrangement of functional domains (Figure 1). These include several regions that come together in the three dimensional structure of the protein to form a GTP/GDP binding pocket, and two so-called 'switch' domains that interact with Rab-effector proteins and undergo a conformational change according the presence of either GDP or GTP. Rab proteins also contain a C-terminal prenylation motif, consisting of the last four amino acids; after translation, lipid modification occurs at this motif following geranylgeranylation, which is essential for targeting of Rabs to specific membranes, and thus for their subsequent function [Pfeffer & Aivazian, 2004]. Whereas most Rab proteins have a dicysteine prenylation motif, that of Rab23 has only a single cysteine residue, more characteristic of the Rho and Ras GTPase families. Because of this, and unlike other Rabs with dicysteine motifs, Rab23 is not trafficked through the secretory pathway [Leung et al., 2007]. Instead, trafficking of Rab23 to the plasma membrane may involve an alternative mechanism involving phospholipids [Heo et al., 2006]. Given the current absence of homozygous point mutations in *RAB23*, it is not yet clear how disruption of these different functional domains contributes to pathogenesis.

As well as disruption of protein function, the other mechanism to be considered in Carpenter syndrome is nonsense-mediated mRNA decay (NMD). NMD is a surveillance mechanism that recognizes and degrades transcripts carrying premature termination codons (PTCs) arising from erroneous transcription or splicing, or that are encoded by splice-site or nonsense/frameshift mutations [Khajavi et al., 2006]. NMD has been shown to modulate human disease phenotypes. For example, the clearance of mutant transcripts by NMD may reduce disease severity by eliminating transcripts that encode proteins with dominant-negative effects. Disease phenotypes associated with NMD may also depend on the position of a PTC within the gene, because PTCs are recognized by the presence of exon junction complexes at downstream exon-exon junctions. Therefore, PTCs may escape NMD if they are located in the final exon or 3′ end of the penultimate exon. For example, nonsense mutations in the final exon of either *HBB* or *SOX10* escape NMD and have dominant-negative effects, thereby giving rise to more severe phenotypes than nonsense mutations located in upstream exons that are subject to NMD [Hall & Thein, 1994; Inoue et al., 2004]. The stability of *RAB23* transcripts carrying PTCs has not previously been investigated.

MATERIALS AND METHODS

Identification of RAB23 mutations

This study was approved by the Oxfordshire Research Ethics Committee B (C02.143) and informed consent was obtained from the parents of affected children. Genomic DNA was extracted from peripheral blood by proteinase K digestion and phenol-chloroform extraction. All coding exons (exons 2-7) of *RAB23*, and their surrounding intronic regions, were sequenced in each patient in both forward and reverse directions as described previously [Jenkins et al., 2007]. Mutation nomenclature is based on http://www.hgvs.org/mutnomen/recs-prot,

and nucleotide numbering of *RAB23* cDNA is based on GenBank sequence NM_183227.1, starting from the first base of the initiation codon.

Analysis of abnormal splicing

Total RNA was extracted from peripheral blood (obtained in PAXgene tubes) using the PAXgene Blood RNA Kit (QIAGEN, Crawley, UK), from which cDNA was prepared by reverse transcription using the RETROscript Kit (Ambion/Applied Biosystems, Warrington, UK). Reverse transcriptase-PCR (RT-PCR) was performed using primers (Forward – 5′-TCGCCATAAAGATGGTGGTTGTAGGGAATG-3′ and Reverse – 5′-GCACAAGTACAGTTGGTATATCTCCCACTTC-3′), located in exons 2 and 4, respectively.

Quantification of NMD by pyrosequencing

To analyze the c.434T>A (p.L145X) mutation, cDNA was prepared from peripheral blood as described above, and a 304 bp RT-PCR product spanning *RAB23* exons 3 to 6 was generated using the following primers: Forward – 5′-GCTTGTGTGCTCGTGTTCTC-3′ and Reverse – 5′-GCGTTAGTTCTGGATCCTCAG-3′. Single-stranded DNA was obtained from 10 µl of each of three independent PCR products by immobilization on streptavidin-coated sepharose beads (Streptavidin Sepharose high performance, GE Healthcare, Chalfont St. Giles, UK), and denaturation using NaOH. Pyrosequencing was performed on a PyroMark Q96 MD (QIAGEN, Crawley, UK) in the reverse direction using the primer 5′-CTGATGTTCTGTAGAATCTT-3′. After dispensation of enzyme (E) and substrate (S), the nucleotides were dispensed in the order A-T-C-A-T-C-G-C-A-T-C-A-C-T-G-C. Dispensations were designed to generate several peaks unique to either mutant or wild-type alleles, as well as blank peaks that were negative for both mutant and wild-type alleles, so as to measure background peak heights. All pyrograms passed the following quality control criteria: (1) mutant-specific peaks were not generated in wild-type cDNA samples (mutant/wild-type (M/WT) ratio <0.05); (2) deliberately blank dispensations did not produce peaks. Following subtraction of blank peaks, M/WT ratios were calculated for peaks generated by the same nucleotide dispensed at similar positions.

RESULTS

As part of our ongoing screening of patients with Carpenter syndrome, we identified a further 10 subjects, from 8 independent families, with biallelic mutations in *RAB23*. A summary of the mutations is presented in Table 1 and Figure 1; associated clinical features are detailed in Supplementary Table S1 and representative clinical photographs are provided in Figure 2. All patients were born to phenotypically normal parents and, when samples were available for analysis, heterozygosity for the identified mutations was confirmed in these parents.

We identified 6 different *RAB23* mutant alleles in this series, all of which are novel except for the common c.434T>A (p.L145X) mutation. p.L145X comprised at least one mutant allele in all 5 families of white north European origin, consistent with the founder effect previously identified in this population. In 3 of these families (subjects 554, 4080 and 4206/7), affected individuals were apparently homozygous. In the other two north European families affected individuals were compound heterozygotes for L145X and a different allele; in one (siblings 4388 and 4389), two different nonsense mutations (p.[R28X;L145X]) were co-inherited from the unaffected mother, in the other (subject 4154) a novel mutation, c.156-3T>G, which causes disrupted splicing, was present (see below).

In each of the three families originating outside of northern Europe, we identified a different, novel homozygous mutation. A patient from Brazil (subject 4121) had a frameshift mutation, p.N121fsX4, similar to others that we described previously. The three other patients had mutations affecting single amino acid residues (subject 4203 from Mexico, c.35T>A encoding p.M12K; siblings 4119 and 4120 from Turkey, c.234_236del encoding p.Y79del). Both mutations are expected to affect protein function on the basis of evolutionary conservation, crystal structure and domain organization of RAB23 (Figure 1 and Supplementary Figure S1; Eathiraj et al., 2005; see *Discussion* below).

The c.156-3T>G mutation present in subject 4154 is located just upstream of exon 3 (Figure 3A). Mutations of the -3 position are a relatively unusual cause of abnormal splicing, but G at -3 is strongly disfavored at 3′ splice sites and precedents exist for this change being pathogenic [Wong et al., 1989]. To determine whether this mutation affects splicing, RT-PCR was performed using primers in exons 2 and 4. Amplification of control *RAB23* cDNA generated a single 336 bp product, as expected for a full-length transcript that includes exon 3. By contrast, analysis of cDNA extracted from peripheral blood obtained from the father (from whom the mutation had been

Table 1. *RAB23* mutations identified in patients with Carpenter syndrome in the current study.

					Mutation at Allele			
					Maternal		Paternal	
Subject	**Sex**	**Parental Consanguinity**	**Country of Origin**	**Sample(s) Analyzed**	**DNA**	**Protein**	**DNA**	**Protein**
4203	F	-	Mexico	P, Mo and Fa	c.35T>A	p.M12K	c.35T>A	p.M12K
4388 (Family 2)	M	-	north European (Australia)	P, Mo and Fa	c.[82C>T; 434T>A]	p.[R28X;L145X]	c.434T>A	p.L145X
4389 (Family 2)	M	-	north European (Australia)	P, Mo and Fa	c.[82C>T; 434T>A]	p.[R28X;L145X]	c.434T>A	p.L145X
4154	M	-	north European (Belgium)	P, Mo and Fa	c.434T>A	p.L145X	c.156-3T>G	p.V53fsX13
4119 (Family 1)	M	1st cousins	Turkey	P, Mo and Fa	c.234_236delCTA	p.Y79del	Same	-
4120 (Family 1)	M	1st cousins	Turkey	P, Mo and Fa	c.234_236delCTA	p.Y79del	Same	-
4121	M	1st cousins	Brazil	P and Mo	c.362_363insG	p.N121fsX4	Same	-
554	F	-	north European (UK)	P	c.434T>A	p.L145X	?	?
4080	M	-	north European (UK)	P	c.434T>A	p.L145X	?	?
4206/7	M	-	north European (Australia)	P, Mo and Fa	c.434T>A	p.L145X	c.434T>A	p.L145X

Abbreviations: F, female; Fa, father; M, male; Mo, mother; P, patient. For cases in which the two parental alleles are unlikely to be independent (owing to documented consanguinity), the paternal allele is denoted "Same". Mutations for which only the patient DNA was available are listed in the Maternal columns, with "?" in the Paternal columns.

inherited), showed an additional smaller product of ~250 bp, consistent with skipping of exon 3 (Figure 3B). Gel purification and direct sequencing confirmed that this smaller fragment comprised exon 4 spliced directly to exon 2, producing an out-of-frame transcript which introduces a PTC (designated r.156_241del, predicting the frameshift mutation p.V53fsX13) (Figure 3C). Notably, the intensity of the 250 bp fragment was significantly less than the 360 bp wild-type fragment, despite its smaller size; this suggests that the mutant transcript is unstable.

To investigate the wider significance of NMD for expression of *RAB23* transcripts, we used pyrosequencing to quantify the relative levels of wild-type and mutant transcripts in the mother of a patient who we previously reported with Carpenter syndrome (subject 3734; [Jenkins et al., 2007]), who was heterozygous for the c.434T>A (p.L145X) allele (Figure 3D). There was a clear reduction in the levels of mutant transcripts compared to wild-type; we determined that transcripts encoding p.L145X were present at 43.8% ± 8.2% (standard error of the mean) of the level of wild-type transcripts, suggesting that the p.L145X allele also confers transcript instability.

DISCUSSION

In this study, we have identified a further 8 families with mutations in the *RAB23* gene, nearly doubling the number of different mutant alleles known. These additional patients have enabled us to establish a clearer picture of the phenotypic spectrum in Carpenter syndrome. We provide the first direct evidence that truncating mutations in *RAB23* are unstable, suggesting a role for NMD in pathogenesis, and describe the first homozygous mutations in *RAB23* that encode single amino acid changes. These mutations are associated with a similar phenotypic spectrum to nonsense mutations, thereby identifying key residues that are essential for protein function.

The cases presented here, together with those previously published by Jenkins et al. [2007] and Alessandri et al. [2010] provide an expanded series in which to examine the phenotypic spectrum of Carpenter syndrome. The only universal features are craniosynostosis and soft-tissue syndactly, usually accompanied by insertional/preaxial

polydactyly of the feet and often postaxial polydactyly of the hands; cryptorchidism/hypoplastic external genitalia were observed in almost all male cases (Supplementary Table S1). Where CT scanning of the skull was performed, fusion of the sagittal suture was observed in all patients, and bicoronal synostosis was almost always present. Whereas all patients in the study by Jenkins et al. [2007] had high birth weight, the birth weights in the current group of patients were in the normal range, although they did go on to exhibit postnatal obesity. Polysplenia/accessory spleens, a characteristic laterality defect, was previously reported by Alessandri et al. [2010] in a single patient. One patient in the present study (subject 4080) exhibited this phenotype, confirming this as a specific association with mutation of *RAB23*, and suggesting a role for RAB23 in the regulation of left-right patterning.

Greig syndrome, which is caused by heterozygous loss-of-function mutations in *GLI3* (MIM*165240), is also characterized by polysyndactyly, as well as other features seen in Carpenter syndrome, including agenesis of the corpus callosum and cryptorchidism in boys [Johnston et al., 2005]. Recently, synostosis of the metopic or sagittal sutures has been reported as a rare association with Greig syndrome [Johnston et al., 2010; Kini et al., 2010; McDonald-McGinn et al., 2010], further confusing accurate diagnosis. Indeed, three patients referred to us for *RAB23* mutation testing proved instead to be positive for 6.0-8.3 Mb deletions including *GLI3* [Hurst et al., under revision]. Currently, only midline synostosis has been reported in Greig syndrome, so the presence of bicoronal synostosis in almost all patients with Carpenter syndrome, together with other frequent features such as obesity and umbilical hernia, help to distinguish between the two disorders. However, patients with either diagnosis should be considered for both *GLI3* and *RAB23* testing.

The identification of a homozygous missense mutation (p.M12K) and a homozygous amino acid deletion (p.Y79del) in RAB23, which were both associated with fairly typical features of Carpenter syndrome, highlights two residues important for normal biochemical function. Like other Rab proteins, the core structure of RAB23 comprises 6 buried β-strands [Eathiraj et al., 2005]. Both the p.M12K mutation (Supplementary Figure S1A) and the previously reported p.C85R mutation [Jenkins et al., 2007], represent non-conservative substitutions from sulfur-containing amino acids located within this core, to charged residues with more bulky side chains. These mutations are therefore likely to disrupt protein folding. The p.Y79del is located within one of the switch domains of RAB23. Both Rab3a and Rab5c contain a triad of hydrophobic residues, including a tyrosine residue in the switch domain, equivalent to Y78 in RAB23, that interact with effector proteins [Merithew et al., 2001]. The Y78 residue is adjacent to the deleted Y79, which normally points in the opposite direction and is conserved in both Rab3a and Rab5c (Supplementary Figure S1B). Therefore, deletion of the Y79 residue is likely to disrupt interaction of RAB23 with effector proteins. Because patients homozygous for both p.M12K and p.Y79del exhibit the full Carpenter syndrome phenotype, it is likely that these mutations result in complete loss-of-function.

Notwithstanding these considerations, most patients with Carpenter syndrome reported to date are homozygous for truncating (nonsense or frameshift) mutations in RAB23. Interestingly, these truncating mutations seem to be distributed unevenly, being absent in the final third of the protein (Figure 1). If the C-terminal prenylation motif of RAB23 were essential for function, as in other Rabs, then truncating mutations located anywhere in the gene would be expected to generate null-alleles. Although further mutation screening will be required to confirm that the spectrum of truncating mutations is non-random, this may be explained by the fact that the prenylation motif of RAB23 is atypical (see *Introduction*). This suggests that alternative mechanisms, other than disruption of prenylation, may also be critical for pathogenesis; NMD represents one such mechanism.

We evaluated NMD by analyzing the relative levels of mutant and wild-type transcripts in individuals heterozygous for *RAB23* mutations, and found that transcripts encoding truncated forms of *RAB23* are unstable. This was demonstrated both for a splice site mutation (PTC located in the third of six coding exons) and for the most 3′ (and most common) mutation in *RAB23* (p.L145X; PTC in fourth coding exon), suggesting that all truncating mutations in Carpenter syndrome are likely to undergo NMD. Because PTCs in the last exon and 3′ part of the penultimate exon of *RAB23* encoding residues downstream of p.L145, are expected to escape NMD [Khajavi et al., 2006], the absence of mutations in this region may also reflect a critical role for NMD in pathogenesis. Although more N-terminally located truncating mutations might be expected to give rise to more severe phenotypes by disrupting more of the functional domains, no genotype-phenotype correlations are apparent with respect to the location of truncating mutations in *RAB23*. This evidence also points to an important role for NMD in pathogenesis.

ACKNOWLEDGMENTS

We thank all patients and their families for participating in this study, and all clinicians who referred patients to us. We also thank Dr. Anne Goriely for advice with pyrosequencing, and other members of the Wilkie lab for help and support.

REFERENCES

Alessandri JL, Dagoneau N, Laville JM, Baruteau J, Hébert JC, Cormier-Daire V. 2010. RAB23 mutation in a large family from Comoros Islands with Carpenter syndrome. Am J Med Genet A 152A:982-6.

Carpenter G. 1901. Two sisters showing malformations of the skull and other congenital abnormalities. Rep Soc Study Dis Child Lond 1:110-118.

Eathiraj S, Pan X, Ritacco C, Lambright DG. 2005. Structural basis of family-wide Rab GTPase recognition by rabenosyn-5. Nature 436:415–419.

Hall GW, Thein S. 1994. Nonsense codon mutations in the terminal exon of the β-globin gene are not associated with a reduction in β-mRNA accumulation - A mechanism for the phenotype of dominant β-thalassemia. Blood 83:2031–2037.

Heo WD, Inoue T, Park WS, Kim ML, Park BO, Wandless TJ, Meyer T. 2006. PI(3,4,5)P3 and PI(4,5)P2 lipids target proteins with polybasic clusters to the plasma membrane. Science 314:1458-61.

Hurst JA, Jenkins D, Vasudevan PC, Kirchhoff M, Skovby F, Rieubland C, Gallati S, Rittinger O, Kroisel PM, Johnson D, Biesecker LG, Wilkie AOM. 2011. Metopic and sagittal synostosis in Greig cephalopolysyndactyly syndrome: five cases with intragenic mutations or complete deletions of *GLI3*. *Eur J Hum Genet*, under revision

Inoue K, Khajavi M, Ohyama T, Hirabayashi S, Wilson J, Reggin JD, Mancias P, Butler IJ, Wilkinson MF, Wegner M, Lupski JR. 2004. Molecular mechanism for distinct neurological pheno-types conveyed by allelic truncating mutations. Nat Genet 36:361–369.

Jenkins D, Seelow D, Jehee FS, Perlyn CA, Alonso LG, Bueno DF, Donnai D, Josifova D, Mathijssen IM, Morton JE, Orstavik KH, Sweeney E, Wall SA, Marsh JL, Nurnberg P, Passos-Bueno MR, Wilkie AOM. 2007. RAB23 mutations in Carpenter syndrome imply an unexpected role for hedgehog signaling in cranial-suture development and obesity. Am J Hum Genet 80:1162-70.

Johnston JJ, Olivos-Glander I, Killoran C, Elson E, Turner JT, Peters KF, Abbott MH, Aughton DJ, Aylsworth AS, Bamshad MJ, Booth C, Curry CJ, David A, Dinulos MB, Flannery DB, Fox MA, Graham JM, Grange DK, Guttmacher AE, Hannibal MC, Henn W, Hennekam RC, Holmes LB, Hoyme HE, Leppig KA, Lin AE, Macleod P, Manchester DK, Marcelis C, Mazzanti L, McCann E, McDonald MT, Mendelsohn NJ, Moeschler JB, Moghaddam B, Neri G, Newbury-Ecob R, Pagon RA, Phillips JA, Sadler LS, Stoler JM, Tilstra D, Walsh Vockley CM, Zackai EH, Zadeh TM, Brueton L, Black GC, Biesecker LG. 2005. Molecular and clinical analyses of Greig cephalopolysyndactyly and Pallister-Hall syndromes: robust phenotype prediction from the type and position of GLI3 mutations. Am J Hum Genet 76:609-22.

Johnston JJ, Sapp JC, Turner JT, Amor D, Aftimos S, Aleck KA, Bocian M, Bodurtha JN, Cox GF, Curry CJ, Day R, Donnai D, Field M, Fujiwara I, Gabbett M, Gal M, Graham Jr JM, Hedera P, Hennekam RC, Hersh JH, Hopkin RJ, Kayserili H, Kidd AM, Kimonis V, Lin AE, Lynch SA, Maisenbacher M, Mansour S, McGaughran J, Mehta L, Murphy H, Raygada M, Robin NH, Rope AF, Rosenbaum KN, Schaefer GB, Shealy A, Smith W, Soller M, Sommer A, Stalker HJ, Steiner B, Stephan MJ, Tilstra D, Tomkins S, Trapane P, Tsai AC, Van Allen MI, Vasudevan PC, Zabel B, Zunich J, Black GC, Biesecker LG. 2010. Molecular analysis expands the spectrum of phenotypes associated with GLI3 mutations. Hum Mutat 31:1142-54.

Kini U, Hurst JA, Byren JC, Wall SA, Johnson D, Wilkie AOM. 2010. Etiological heterogeneity and clinical characteristics of metopic synostosis: evidence from a tertiary craniofacial unit. Am J Med Genet 152A:1383-9.

Khajavi M, Inoue K, Lupski JR. 2006. Nonsense-mediated mRNA decay modulates clinical outcome of genetic disease. Eur J Hum Genet 14:1074-81.

Leung KF, Baron R, Ali BR, Magee AI, Seabra MC. 2007. Rab GTPases Containing a CAAX Motif Are Processed Post-geranylgeranylation by Proteolysis and Methylation. J Biol Chem 282:1487–1497.

McDonald-McGinn DM, Feret H, Nah HD, Bartlett SP, Whitaker LA, Zackai EH. 2010. Metopic craniosynostosis due to mutations in GLI3: A novel association. Am J Med Genet A 152A:1654-60.

Merithew E, Hatherly S, Dumas JJ, Lawe DC, Heller-Harrison R, Lambright DG. 2001. Structural plasticity of an invariant hydrophobic triad in the switch regions of Rab GTPases is a determinant of effector recognition. J Biol Chem 276:13982-8.

Pfeffer S, Aivazian D. 2004. Targeting Rab GTPases to distinct membrane compartments. Nat Rev Mol Cell Biol 5:886-896.

Wong C, Antonarakis SE, Goff SC, Orkin SH, Forget BG, Nathan DG, Giardina PJV, Kazazian HH. 1989. Beta-thalassemia due to 2 novel nucleotide substitutions in consensus acceptor splice sequences of the beta-globin gene. Blood 73: 914-8.

FIGURE LEGENDS

Figure 1. Mutation spectrum in *RAB23*.
At top, the exon/intron organization of *RAB23,* with the coding part of the cDNA in black and the untranslated regions (UTRs) in white (only exons 2-7 are shown; alternatively spliced 5′ noncoding exons are omitted). Upright numbering refers to the first nucleotide of each exon, starting from the initiation codon, and italic numbering indicates the length of introns. Below, the functional domains in the protein are depicted according to the key. The location of all human mutations described to date that cause Carpenter syndrome are indicated by arrowheads. Black and white arrowheads refer to mutations reported by Jenkins et al. [2007] and Alessandri et al. [2010], respectively. Grey arrowheads refer to novel alleles reported in the current study, and mutations affecting single amino acids are underlined. The asterisk refers to the fact that the p.R28X mutation was co-inherited with the p.L145X mutation, giving a p.[R28X;L145X] allele. Nucleotide numbering reflects cDNA numbering with +1 corresponding to the A of the ATG translation initiation codon in the reference sequence, according to journal guidelines (www.hgvs.org/mutnomen). The initiation codon is codon 1.

Figure 2. Clinical appearance of *RAB23* mutation-positive Carpenter syndrome at different ages.
(A-C) Subject 4388, pregnancy terminated at 19.5 weeks' gestation. **(D-I)** Childhood pictures of subjects 4206/7 aged 3 days **(D,E)**, 4203 aged 11 mo **(F)** and 3 yr **(G)** and 4119 aged 7 yr **(H,I)**. **(J,K,L)** Subject 4121 aged 29 years. Note dysmorphic craniofacial appearance **(A,D,J)** and variable combinations of polydactyly, syndactyly and brachydactyly **(B,C,H,I,K,L)**. However polysyndactyly was absent in subject 4203 homozygous for the p.M12K missense mutation **(F,G)**.

Figure 3. Analysis of transcripts encoded by a splice-site or nonsense mutation.
(A) Sequencing of genomic DNA from subject 4154 showing a heterozygous T>G substitution (arrowhead) 3 bp upstream of exon 3. **(B)** RT-PCR with primers in exons 2 and 4 using cDNA extracted from fresh blood of the father of subject 4154. As well as a wild-type fragment at 336 bp, a second fragment is also observed at 250 bp, which is absent in control cDNA. Note that the smaller fragment is much weaker than the wild-type product. **(C)** Sequencing of the 250 bp fragment, demonstrating skipping of exon 3 in the cDNA product. (**D**) Pyrosequencing assay used to measure the relative levels of c.434T>A (p.L145X) mutant and wild-type transcripts. The dispensation order and peaks for comparison are indicated, below which is a table listing the sequence of nucleotides incorporated into mutant and wild-type transcripts, and the position at which each peak is produced (for example T2 indicates that a T is incorporated at the second dispensation). Representative pyrograms are shown using cDNA originating from peripheral blood of a wild-type individual (left) and a parent heterozygous for the mutation (right). Pairs of arrows link peaks (black: wild-type; grey, mutant) used for comparative quantification.

Supplementary Figure S1. Location of residues altered by homozygous mutations of single amino acids in *RAB23*.
(**A**) Crystal structure of RAB23 (Protein Databank accession 1Z22) showing the location of the p.M12K mutation in the first β-strand (red arrow). Below, the p.M12 residue (highlighted in red) is conserved as an uncharged amino acid in *Homo sapiens* (Hs), *Mus musculus* (Mm), *Danio rerio* (Dr) and *Drosophila melanogaster* (Dm). (**B**) Same crystal structure of RAB23 rotated compared to **A** to show three residues (Y78; W63; F46) that form a hydrophobic triad that interacts with effector proteins (white arrows); p.Y79 is indicated by the red arrow. Below, the p.Y79 residue (highlighted in red) and surrounding amino acids are highly conserved in evolution.

Figure 1.

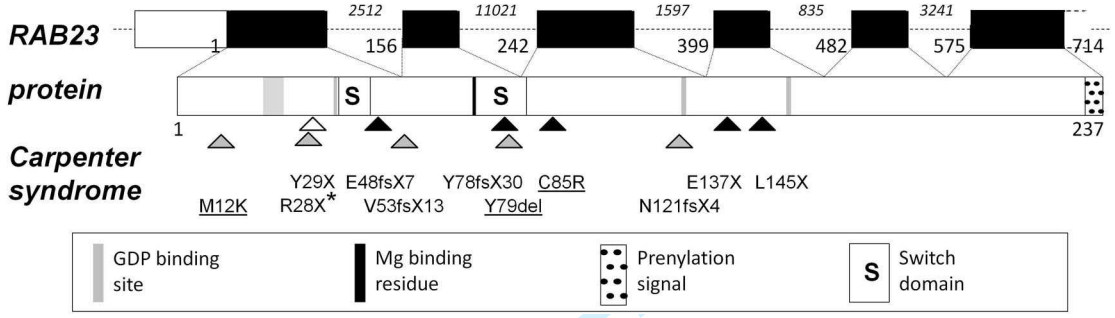

Figure 2.

Figure 3.

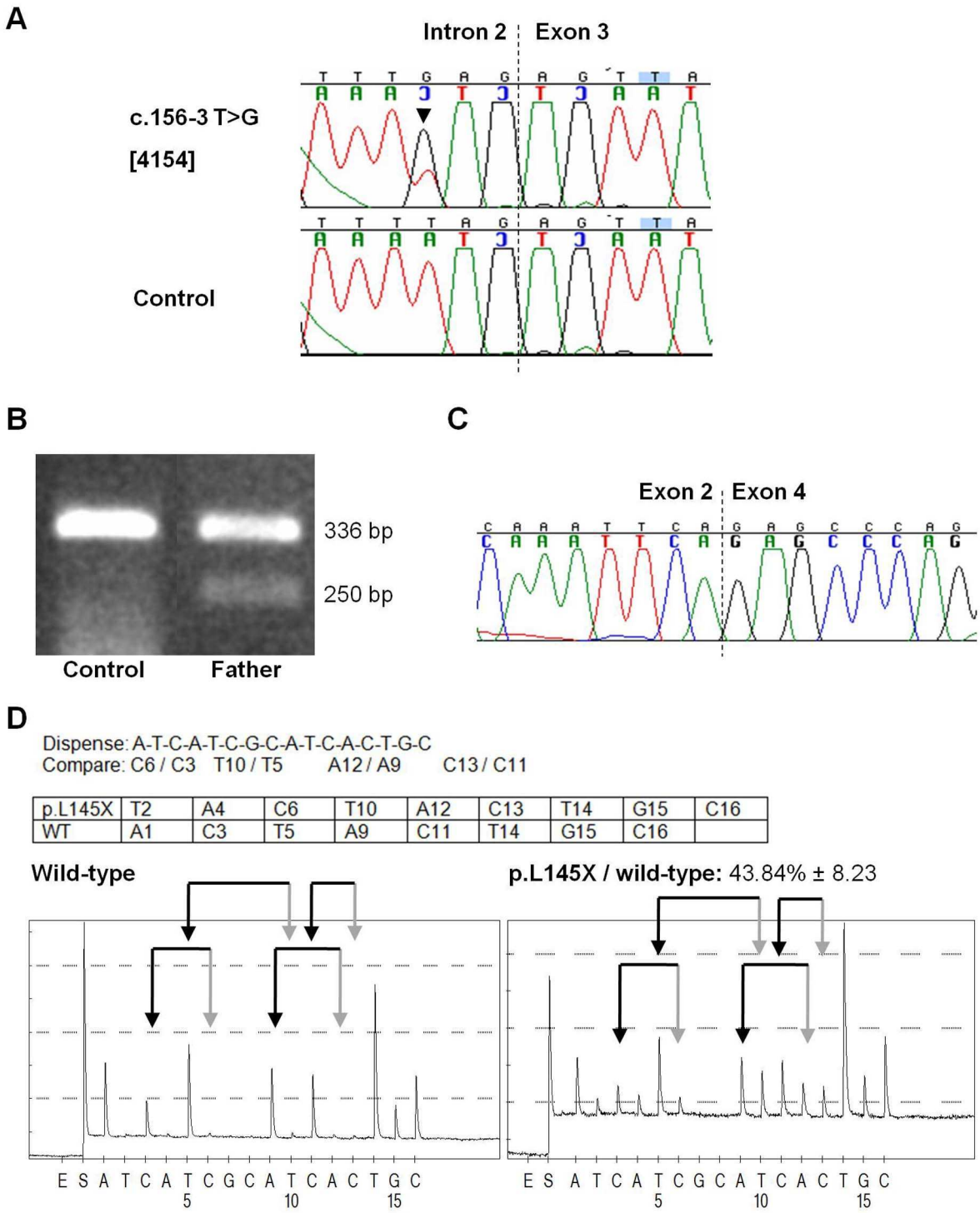
A
Intron 2
Exon 3
c.156-3 T>G
[4154]
Control
B
336 bp
250 bp
Control
Father
C
Exon 2
Exon 4
D
Dispense: A-T-C-A-T-C-G-C-A-T-C-A-C-T-G-C
Compare: C6 / C3 T10 / T5 A12 / A9 C13 / C11
p.L145X T2 A4 C6 T10 A12 C13 T14 G15 C16
WT A1 C3 T5 A9 C11 T14 G15 C16
Wild-type
p.L145X / wild-type: 43.84% ± 8.23
E S A T C A T C G C A T C A C T G C
5
10
15

Supplementary Figure S1.

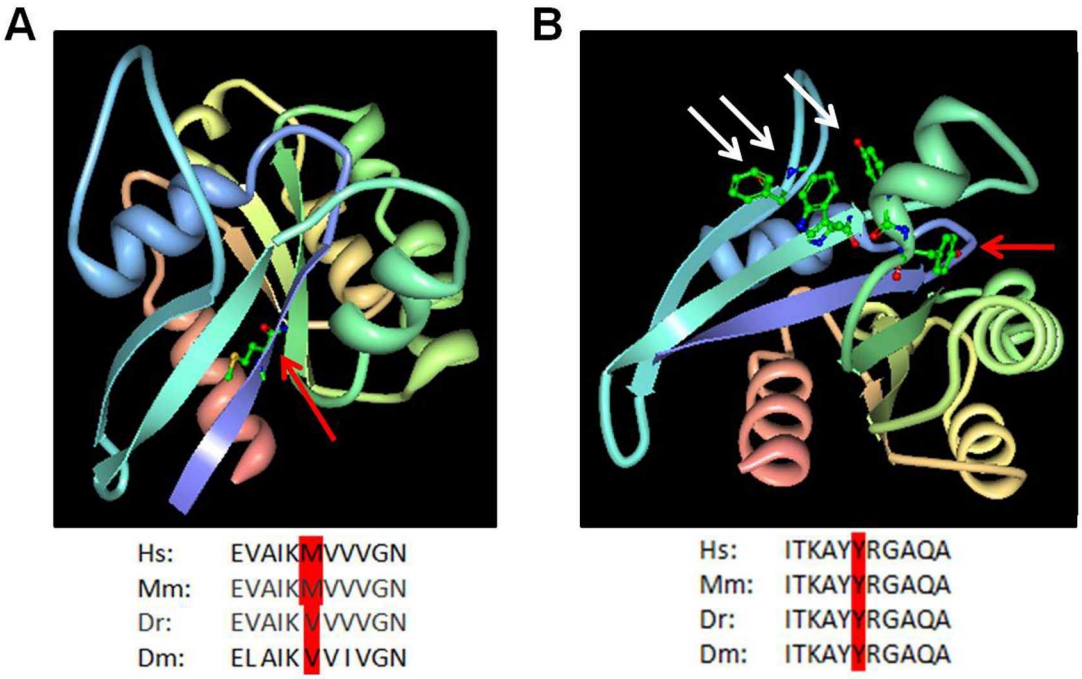

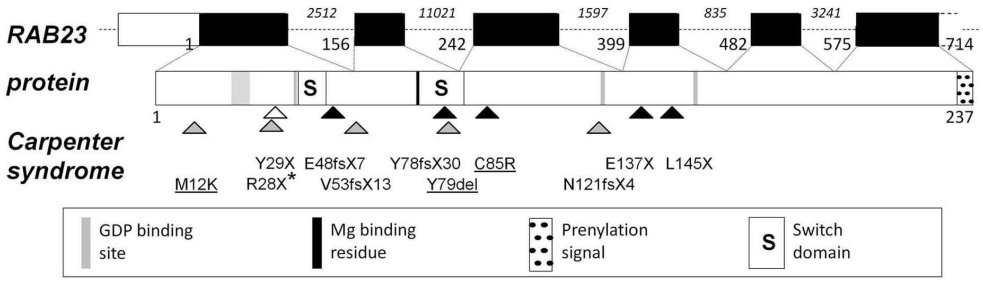

Figure 1. Mutation spectrum in RAB23.
At top, the exon/intron organization of RAB23, with the coding part of the cDNA in black and the untranslated regions (UTRs) in white (only exons 2-7 are shown; alternatively spliced 5′ noncoding exons are omitted). Upright numbering refers to the first nucleotide of each exon, starting from the initiation codon, and italic numbering indicates the length of introns. Below, the functional domains in the protein are depicted according to the key. The location of all human mutations described to date that cause Carpenter syndrome are indicated by arrowheads. Black and white arrowheads refer to mutations reported by Jenkins et al. [2007] and Alessandri et al. [2010], respectively. Grey arrowheads refer to novel alleles reported in the current study, and mutations affecting single amino acids are underlined. The asterisk refers to the fact that the R28X mutation was co-inherited with the L145X mutation, giving an (R28X; L145X) allele.

160x46mm (300 x 300 DPI)

Figure 2. Clinical appearance of RAB23 mutation-positive Carpenter syndrome at different ages. (A-C) Subject 4388, pregnancy terminated at 19.5 weeks' gestation. (D-I) Childhood pictures of subjects 4206/7 aged 3 days (D,E), 4203 aged 11 mo (F) and 3 yr (G) and 4119 aged 7 yr (H,I). (J,K,L) Subject 4121 aged 29 years. Note dysmorphic craniofacial appearance (A,D,J) and variable combinations of polydactyly, syndactyly and brachydactyly (B,C,H,I,K,L). However polysyndactyly was absent in subject 4203 homozygous for the p.M12K missense mutation (F,G).

500x500mm (300 x 300 DPI)

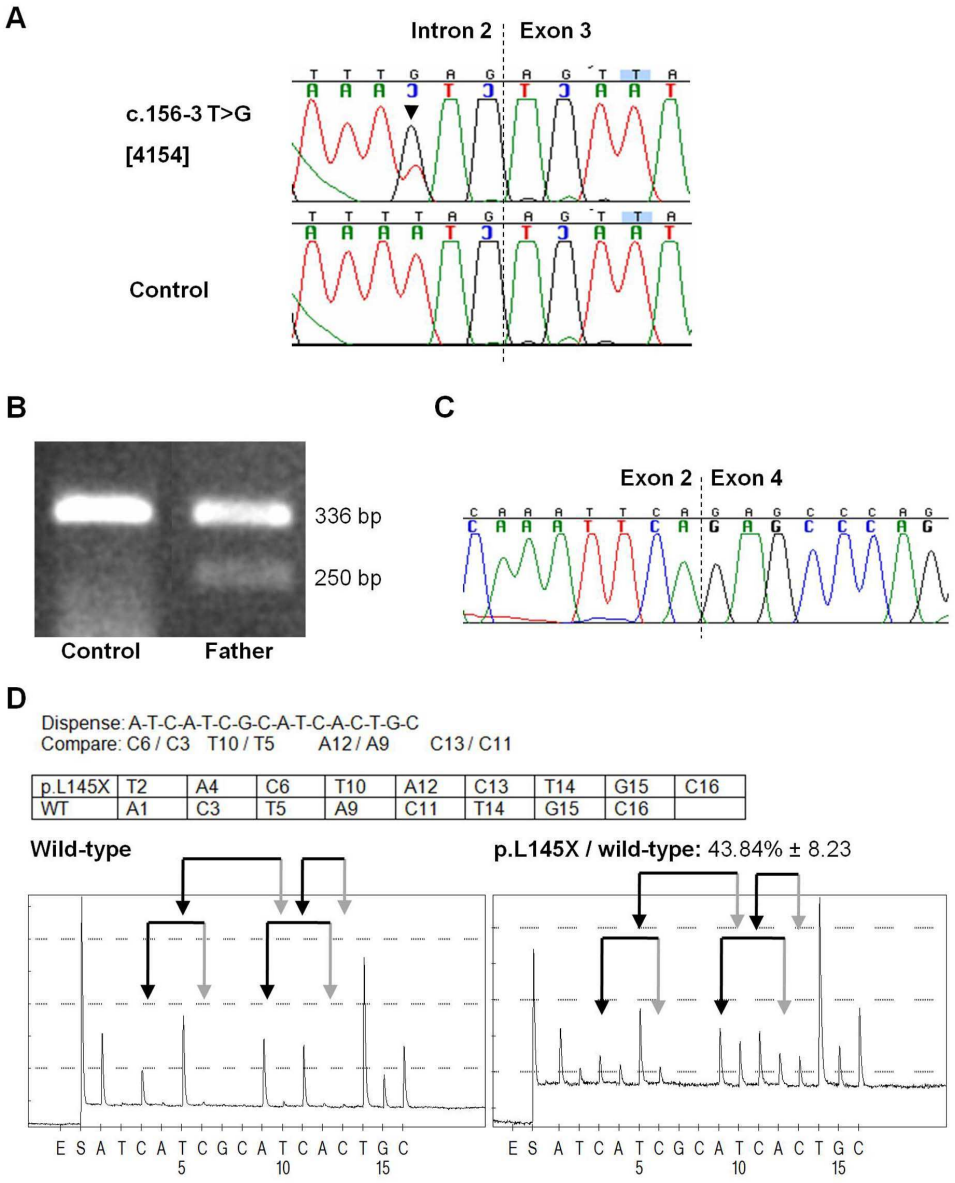

Figure 3. Analysis of transcripts encoded by a splice-site or nonsense mutation. (A) Sequencing of genomic DNA from subject 4154 showing a heterozygous T>G substitution (arrowhead) 3 bp upstream of exon 3. (B) RT-PCR with primers in exons 2 and 4 using cDNA extracted from fresh blood of the father of subject 4154. As well as a wild-type fragment at 336 bp, a second fragment is also observed at 250 bp, which is absent in control cDNA. Note that the smaller fragment is much weaker than the wild-type product. (C) Sequencing of the 250 bp fragment, demonstrating skipping of exon 3 in the cDNA product. (D) Pyrosequencing assay used to measure the relative levels of c.434T>A (p.L145X) mutant and wild-type transcripts. The dispensation order and peaks for comparison are indicated, below which is a table listing the sequence of nucleotides incorporated into mutant and wild-type transcripts, and the position at which each peak is produced (for example T2 indicates that a T is incorporated at the second dispensation). Representative pyrograms are shown using cDNA originating from peripheral blood of a wild-type individual (left) and a parent heterozygous for the mutation (right). Pairs of arrows link

peaks (black: wild-type; grey, mutant) used for comparative quantification.

160x195mm (300 x 300 DPI)

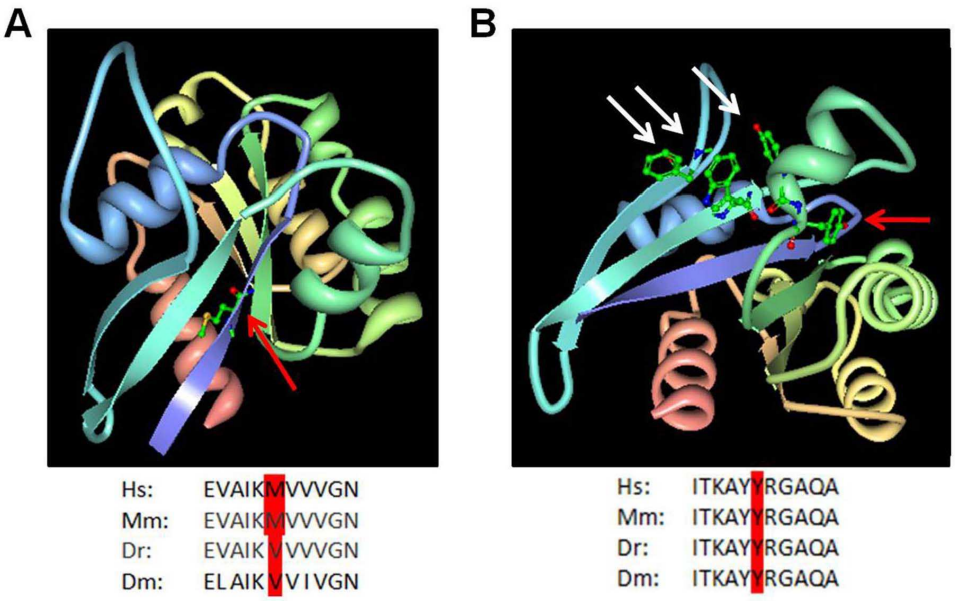

Supplementary Figure S1. Location of residues altered by homozygous mutations of single amino acids in RAB23.
(A) Crystal structure of RAB23 (Protein Databank accession 1Z22) showing the location of the p.M12K mutation in the first β-strand (red arrow). Below, the p.M12 residue (highlighted in red) is conserved as an uncharged amino acid in Homo sapiens (Hs), Mus musculus (Mm), Danio rerio (Dr) and Drosophila melanogaster (Dm). (B) Same crystal structure of RAB23 rotated compared to A to show three residues (Y78; W63; F46) that form a hydrophobic triad that interacts with effector proteins (white arrows); p.Y79 is indicated by the red arrow. Below, the p.Y79 residue (highlighted in red) and surrounding amino acids are highly conserved in evolution.

160x99mm (300 x 300 DPI)

Supplementary Table S1. Clinical features of subjects with mutations in *RAB23*

	ID	Sex	Genotype (nucleotide change above; amino acid change below)	Reported Consanguinity	Ethnicity	Birth weight (g)	Cranial suture fusion	Hydrocephalus	CNS malformation(s)	Preaxial (hand)	Polydactyly (L/R) Postaxial hand	Foot	Additional syndactyly (H/F)	Biphalangeal digits (H/F)	Camptodactyly hands	Talipes/clubfoot	Umbilical hernia	Cardiac malfomation	Urogenital malformation	Other	Height (cm)	Weight (kg)	Age (yr)
1																							
2	4203	F	c.[35T>A]+[35T>A] p.[M12K]+[M12K]	-	Mexican	3900	s,m	+	-		-	-	F (mild)	-H; brachydactyly, F	+	-	-	PDA, VSD, PFO	- (female)	Obese		>97%	
3																							
4																							
5																				Bowed femorae, fused palpebral fissures,			
6	Family 2	4388	M c.[82C>T;434T>A]+[434T>A] p.[R28X;L145X]+[L145X]	-	north European (Australia)		s,bc,bl	-	-	broad thumbs	l,r	l,r	H,F	?; brachydactyly, index finger	+	-	(can't assess-prenatal)	-	-	opaque cornea	25	0.455	19.5/40 wk
7																							
8																							
9																				fused palpebral fissures,			
10	Family 2	4389	M same	-	north European (Australia)		s,bc	-	-	broad thumbs	r	l,r	H,F	?; brachydactyly, R index F		+,L	(can't assess-prenatal)	-	-	opaque cornea	21	0.255	17/40 wk
11																							
12																							
13	4154	M	c.[156-3T>G]+[434T>A] p.[I51fsX14]+[L145X]	-	north European (Belgium)		s,bc	-	-	preaxial polydactyly	l,r	l,r	H,F	+H,F	-	-	(can't assess-prenatal)	-	Cryptorchidism		35.5	1.032	24/40 wk
14																							
15																							
16																							
17																							
18			c.[234_236delCTA]+[234_236delCTA]						Chiari type I malformation, 4th ventricle elongated caudally, ectopic cerebellar tonsil; ventriculo-peritoneal													26 (80th	
19	Family 1	4119	M p.[Y79del]+[Y79del]	1st cousins	Turkish	3000	mu	+	shunt		l,r	l,r	F	-	+	+	-	-	Cryptorchidism	-		centile)	7
20																							
21																							
22									severe hydrocephalus, widened basal cisterns and sylvian											Truncal obesity,		59 (>97th	
23	Family 1	4120	M same	1st cousins	Turkish		dolichocephaly	+	fissures		l,r	l,r	F	-	-	+	-	-	Cryptorchidism	gynaecomastia	148	centile)	11
24			c.[362_363insG]+[362_363insG]																			94 (>97th	
25	4121	M	p.[N121fsX4]+[N121fsX4]	1st cousins	Brazil	3800	+	-	-		-	+	H,F	-	-	-	-	-	Cryptorchidism	Patella/knee problems	141	centile)	29
26																							
27																							
28																							Died aged 26 years,
29	554	F	c.[434T>A]+[434T>A] p.[L145X]+[L145X]	-	north European (UK)		mu			duplicated thumbs	-	l,r	F	+H,F		-	+	Mitral valve prolapse, VSD	-	Left renal hypoplasia			cause unknown
30																							
31																							
32																							
33											l,r									Pinpoint accessory spleens adjacent to normal spleen,			
34	4080	M	c.[434T>A]+[434T>A] p.[L145X]+[L145X]	-	north European (UK)		s,bc		-		(insertional)	l,r	H,F	?; brachydactyly, H,F	+	-	(can't assess-prenatal)	-	Hypoplastic external genitalia	mildly short femurs	29	0.628	22/40 wk
35																							
36																							
37									Agenesis corpus callosum, cerebellar hypoplasia, ventriculomegaly; ventriculo-peritoneal														Died aged 3 years, complicati
38																							
39	4206/7	M	c.[434T>A]+[434T>A] p.[L145X]+[L145X]	-	north European (Australia)	3395	mu	+	shunt	broad, medially deviated thumbs	l,r	l,r	H,F	?; brachydactyly, F	+ (L)	-	-	-	Cryptorchidism				ons of craniosynostosis
40																							

Abreviations:
l - left
r - right
H - hand
F - foot
s - sagital
m - metopic
bc - coronal
bl - bilambdoid
mu - multiple
PDA - patent ductus arteriosus
VSD - ventricular septal defect
PFO - patent foramen ovale

Neurodevelopment
Moderate developmental delay
Severe global developmental delay, epilepsy
Severe global developmental delay
Developmental delay
Normal
Severe global developmental delay